

Simulation of lepton flux at satellite and balloon altitudes

L. Derome and M. Buénerd

Institut des Sciences Nucléaires, IN2P3/CNRS, 53 av. des Martyrs, 38026 Grenoble cedex, France

Abstract. A simulation study of the e^+ and e^- particle flux below the geomagnetic cutoff at satellite and balloon altitudes is reported. The large e^+ over e^- flux asymmetry reported recently by the AMS experiment appears to be due to the geomagnetic East-West effect. Simulation results at various altitudes are compared to data.

1 Introduction

This contribution reports on the results of a simulation study of the electron and positron flux at satellite (≈ 370 km) and balloon altitudes (≈ 35 km). The results are preliminary for the latter. The initial purpose of the study was to reproduce consistently the recent AMS measurements (AMS, 2000a), which were successfully interpreted in a previous publication (Derome L. et al., 2001), referred to as I below. These calculations are complemented in the present report, with the contribution of the incident cosmic ray (CR) ${}^4\text{He}$ to the lepton yield.

The investigation has also been extended to balloon altitude experiments since the problem is the same as for satellite altitude, and the requirement of reproducing both sets of data is more constraining for the calculations. New balloon data have been reported recently by the TS93 (Golden R.L. et al., 1996), CAPRICE (Barbiellini G. et al., 2000b), and HEAT (Barwick S.W. et al., 1998), experiments, whereas some data were available from former measurements, with or without electron-positron discrimination (Israel M. H. (1969); Schmoker J.W. and Earl J.A. (1965); Verma S.D. (1967)).

2 Simulation program

The study was based on the same simulation program for the lepton production and propagation, as used in I (see also Derome L. et al. (2000)). The pion production cross sections in $p + A$ and ${}^4\text{He} + A$ collisions (A atmospheric nu-

clei), the subsequent decays $\pi \rightarrow \mu \rightarrow e$ and $\pi_0 \rightarrow \gamma\gamma$, the lepton Bremstrahlung and the pair conversion cross sections, $\gamma + A \rightarrow e^+e^- + A$ (A atomic nucleus), are implemented in the event generator of the program. Incident CR (p , ${}^4\text{He}$, e^+ , e^-) are generated according to their natural abundance using the recent AMS measurements (AMS, 2000a,c,d). For ${}^4\text{He} + A$ collisions, the pion production was generated assuming the same momentum distribution as in $p + A$ collision, the yield being renormalized to take into account the larger total reaction cross section for ${}^4\text{He}$ (Letaw J.R. et al., 1983; Jaros J. et al., 1978), and the larger pion multiplicity (Agakishiyev H.N. et al., 1985). The contributions of the other CR components, ${}^{12}\text{C}$, ${}^{16}\text{O}$, etc, was neglected. Particles are propagated in the earth magnetic field and atmosphere, and allowed to interact with atmospheric nuclei. Each interaction can produce nucleons and pions according to their respective production cross sections and multiplicities. Each produced particle is then processed the same way, leading to the possible development of atmospheric cascades, in which each particle history is traced and recorded in the program. The e^+ and e^- populations are generated by counting particles each time they cross upwards or downwards the detector altitude within the angular acceptance of the detector. The leptons observed below the Geomagnetic Cutoff (subGC) originate from pion production, either from the decay of secondary charged pions produced in $p + A \rightarrow \pi + X$ collisions, or from pair conversion of gammas, either decaying from neutral pions produced in the same reactions, or radiated by electron Bremstrahlung (see I). The pion production cross-sections are then a critical input to the calculations. The way they are calculated is described in I and in (Liu Yong et al., 2001a). Note that these calculations do not include any adjustable parameters.

Correspondence to: L. Derome (derome@isn.in2p3.fr)

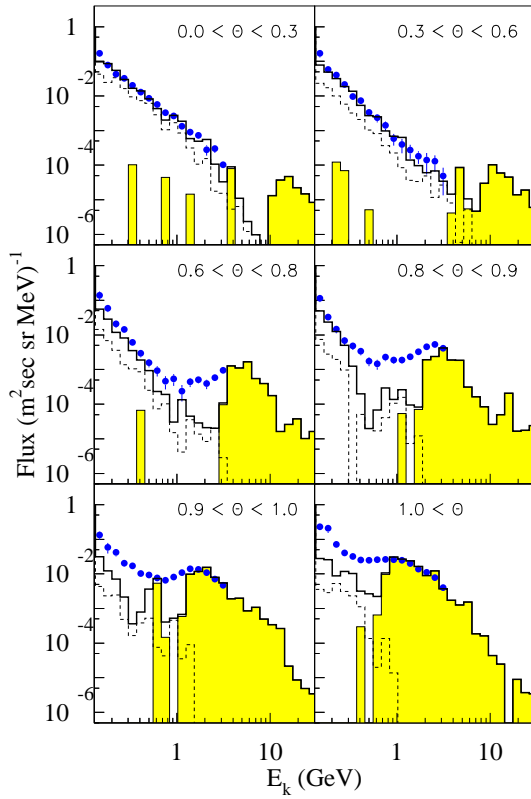


Fig. 1. AMS data and simulation results for the downward electron flux.

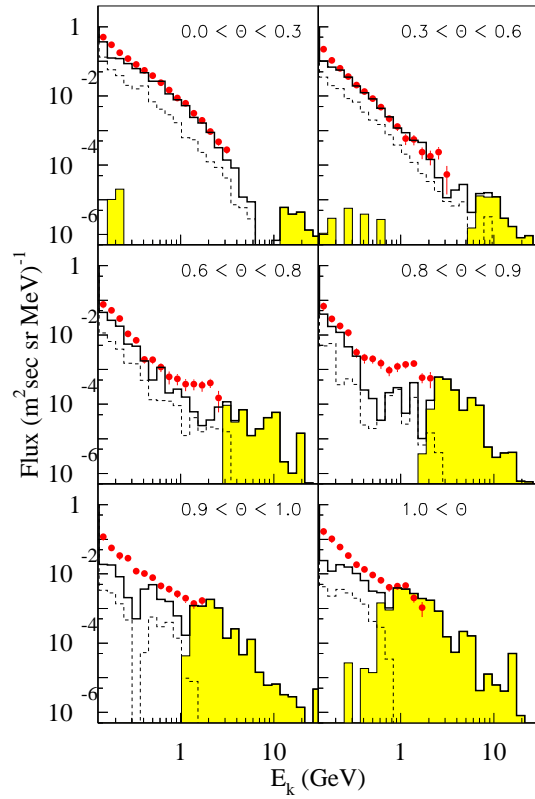


Fig. 3. Downward positron flux.

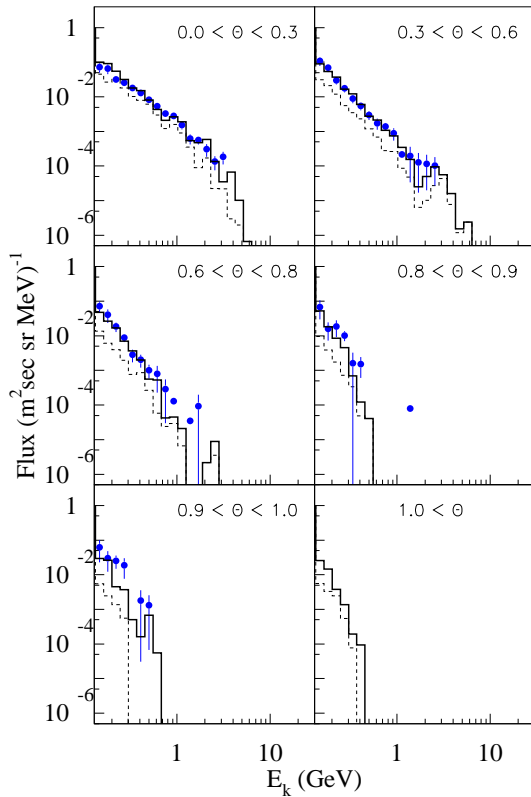


Fig. 2. Upward electron flux.

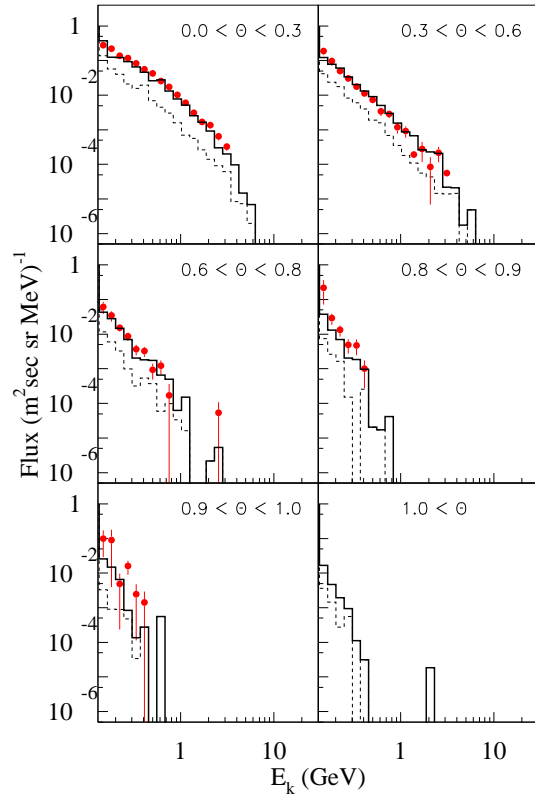


Fig. 4. Upward positron flux.

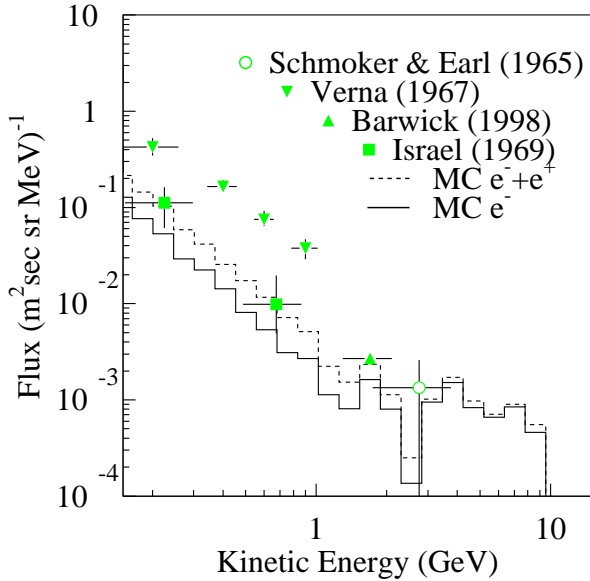


Fig. 5. Downward electron flux measured at 35 km altitude (6 g/cm² atmospheric depth, see table 1), compared with simulation results for e^- (solid line) and $e^+ + e^-$ (dashed line), calculated for $0.6 < \theta_M < 0.8$ CGM latitude.

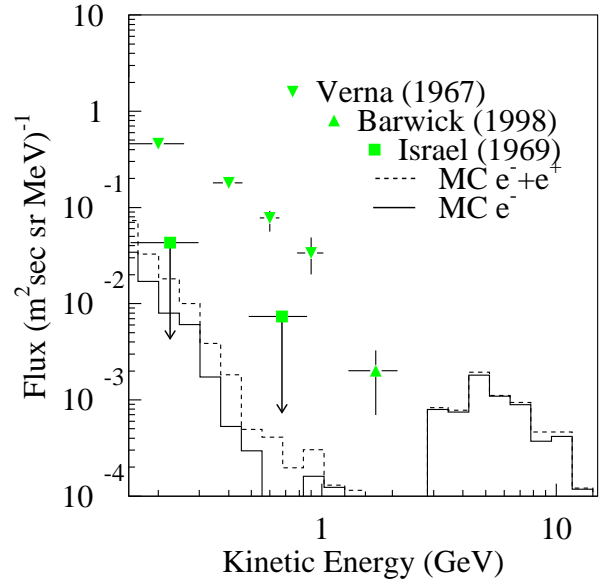


Fig. 6. Downward electron flux at TOA, from data extrapolation (see table 1), compared with simulation results for e^- (solid line) and $e^+ + e^-$ (dashed line), calculated at 70 km altitude (< 0.1 g/cm²) and for $0.6 < \theta_M < 0.8$ CGM latitude.

3 Results

3.1 AMS measurements

The same simulation program has been used to simulate the production of a number of other particle species at satellite (AMS) altitude: protons (Derome L. et al., 2000), light nuclei (Derome L. and Buénerd, M., 2001), and muons and neutrinos (Liu Yong et al., 2001b). All secondary particle distributions obtained are in good agreement with the data. In I, the remarkable features of the lepton distributions observed by AMS: low energy (subGC) spectra, positron over electron ratio, and their dependence on latitude, could be well reproduced by the calculations (Derome L. et al., 2001).

Figures 1,2,3,4 show the e^- and e^+ downward and upward spectra measured by AMS (AMS, 2000a) compared with the results of the simulation (histograms), below and above GC, for the same bins of geomagnetic latitudes. The full line histograms correspond to the total flux calculated for proton plus ^4He incoming CR flux, the shaded area corresponding to the CR flux, while the dashed histograms show the single ^4He contribution. The latter is seen to be quite significant since it amounts to about 40% or even more, of the total yield for all latitudes. This is due to the larger reaction cross section and also to the much larger pion multiplicity (by a factor of about 3 (Agakishiyev H.N. et al., 1985)), for ^4He induced reactions than for proton induced reactions.

The two lepton populations below GC are seen to be very well reproduced both for downward and upward leptons, in the equatorial region as well as at intermediate latitudes. In the polar region however, the simulated flux somewhat un-

derestimates the experimental flux of secondaries for both e^- and e^+ . Note that the latter is a most difficult spectrum to account for since in absence of GC at this latitude, the incident energy range of CR protons covers a very large energy domain, basically from around threshold (about 500 MeV) up to several 10^2 GeV. See I for details and the origin of the electron positron asymmetry.

3.2 Balloon measurement

Measurements of subGC electron flux were made over several decades in a series of high-altitude balloon flights. Table 1 shows a sample of balloon experiments performed at approximately equal CGM latitudes (around 0.7 rad) and at the same altitude (4-6 g/cm² of residual atmosphere). For some of these experiment the apparatus used had no e^+/e^- discrimination capability (see last column of table 1).

Figure 5, shows the experimental values for the downward electron flux, compared with the simulation results at the measurement altitude, 35 km (6 g/cm²). The agreement between simulation results (electron+positron) and the values measured by Israel M. H. (1969) which had no lepton charge discrimination, is very good. It is also fair for the electron data point from Barwick S.W. et al. (1998) (to be compared with the full line histogram) although the experimental value is somewhat underestimated. The incompatibility of the data from Verma S.D. (1967) with those quoted before has been noted previously by Israel M. H. (1969).

In order to obtain the trapped electron population, the measured values from figure 5 have been corrected in the original works, from atmospheric absorption and production, and

Reference	Geographic location	Date of experiment	Latitude (rad)	Depth (g/cm ²)	e^+/e^- ID
Verma S.D. (1967)	Palestine, Tx	1965	0.72	4.	no
Israel M. H. (1969)	Palestine, Tx	1967	0.72	5.2	no
Barwick S.W. et al. (1998)	Fort Summer, NM	1998	0.74	4-7	yes
Schmoker J.W. and Earl J.A. (1965)	San Angelo, Tx	1962	0.77	6.	yes

Table 1. Sample of high-altitude middle latitude ballon experiments used in this work. Latitude is CGM. The last two columns give the altitude in atmospheric depth and the identification capability of the experiment for e^+/e^- discrimination. The measurement from Barwick et al., used here was for 5.5 g/cm² (see figure 5).

evaluated at the top of atmosphere (TOA). The result from this extrapolation are compared on figure 6 with the simulation results at 70 km altitude, i.e., less than .1 g/cm² of residual atmosphere, a good approximation of TOA. The trapped and primary contributions are seen as low and high energy component respectively in the simulated spectrum. The calculated values are compatible with the upper limits from Israel M. H. (1969), although smaller than the upper energy value around 0.7 GeV by more than one order of magnitude. Conversely, the simulated value in the 2 GeV region, is in sharp disagreement with the experiment extrapolation, and close to 2 orders of magnitude smaller. Work is in progress to understand this discrepancy.

4 Conclusion

In conclusion, it has been shown that the e^+ and e^- populations measured by AMS below the geomagnetic cutoff can be well reproduced by simulation assuming the production to originate from the hadronic production of π^+ and π^- in CR($p + {}^4He$)-atmosphere interaction. The same calculations are also in fairly good and then consistent agreement with balloon data, showing the reliability of the calculations.

References

- Agakishiyev H.N. et al., *Z. Phys.* C27(1985)177
The AMS collaboration, Alcaraz J. et al., *Phys. Lett.* B484, 10, 2000a.
The AMS collaboration, Alcaraz J. et al., *Phys. Lett.* B472, 215, 2000b.
The AMS collaboration, Alcaraz J. et al., *Phys. Lett.* B490, 27, 2000c.
The AMS collaboration, Alcaraz J. et al., *Phys. Lett.* B494, 19 2000d.
Derome L. et al., *Phys. Lett.* B 489, 1, 2000
Derome L., Liu Yong and Buénerd M., *Phys. Lett. B*, in press; astro-ph/0103474, March 2001
Derome L. and Buénerd M., 27th ICRC, Hamburg, Aug 7-14, 2001, these proceedings.
Barwick S.W. et al., *J. Geophys. Res.* 103, 4817, 1998
Barbiellini G. et al., 25th ICRC conf, Durban, Aug 1997, OG7.1.5
Golden R.L. et al., *ApJ* 436, 769, 1994
Golden R.L. et al., *ApJ* L457, 103, 1996
Israel M. H., *J. Geophys. Res.* 74, 4701, 1969.
Jaros J., et al., *Phys. Rev.* C18, 2273, 1978
Letaw J.R., Silberberg R., and Tsao C.H., *Ap.J. Suppl.* 51, 271, 1983
Liu Yong, Derome L., and Bunerd M., internal report ISN-01-12, march 2001a.
Liu Yong, Derome L., and Buénerd M., 27th ICRC, Hamburg, Aug 7-14, 2001b, these proceedings.
Schmoker J.W., and Earl J.A., *Phys. Rev.* 138, 300, 1965.
Verma S.D., *J. Geophys. Res.* 72, 915, 1967.